
Article:
Carslaw, Nicola orcid.org/0000-0002-5290-4779, Shaw, David orcid.org/0000-0001-5542-0334, Kruza, Magdalena et al. (1 more author) (2021) Towards improved models for indoor air chemistry: a Monte Carlo simulation study. Atmospheric Environment. 118625. ISSN 1352-2310

https://doi.org/10.1016/j.atmosenv.2021.118625

Atmospheric Environment 262 (2021) 118625

Contents lists available at ScienceDirect

Atmospheric Environment

journal homepage: www.elsevier.com/locate/atmosenv

Towards improved models for indoor air chemistry: A Monte Carlo simulation study

Magdalena Kruza [a], David Shaw [a], Jacob Shaw [b], Nicola Carslaw [a,*]

[a] Department of Environment and Geography, University of York, Wentworth Way, York, YO10 5NG, United Kingdom
[b] Centre for Atmospheric Science, Department of Earth and Environmental Science, University of Manchester, Oxford Road, Manchester, M13 9PL, United Kingdom

HIGHLIGHTS

- Monte Carlo simulations of indoor air concentrations rank input parameter importance.
- Air exchange and ozone deposition control O3, RO2, HO2 and PAN species concentrations.
- Accurate UV transmission/O3 deposition values reduce model uncertainty by up to 80%.
- Increasing UV transmission reduces NO2/HONO concentrations, but increases those of organic nitrates/PAN species.

ARTICLE INFO

Keywords:
Indoor air chemistry
INDCM
Hydroxyl radical
Input parameters
Monte Carlo analysis

ABSTRACT

Model predictions are sensitive to a number of complex and often coupled input parameters. Some of these parameters have a wide range of acceptable values from literature and therefore choosing the appropriate value is non-trivial. In this paper, we use the INdoor Detailed Chemical Model (INDCM) to perform a Monte Carlo analysis, in which a wide but realistic range of model input parameter values is stochastically varied over 1000 model runs. The model output defines the likely range of the model performance, and directly correlates input parameter values with predicted indoor air species concentrations. The air exchange rate or the ozone deposition velocity onto internal materials such as painted walls, control the predicted concentrations of ozone, hydroxyl and peroxy radicals and peroxyacetyl nitrate species for our study conditions. The transmission of UV light from outdoors showed the strongest Spearman's rank positive correlation coefficients with predicted hydroxyl radical (0.92), and organic nitrate (0.95) concentrations. The deposition rate of ozone onto painted walls shows the strongest negative correlations with 4-oxopentanal (−0.86) and acetic acid (−0.83). Reducing the uncertainty around transmission of UV light indoors and ozone deposition rates onto surfaces reduces the model uncertainty by up to 70–80% for ozone and hydroxyl radical concentrations. Some species concentrations showed complex relationships with the various input parameters. For instance, maximum isoprene concentrations decreased with air exchange rate, but minimum isoprene concentrations were largely invariant. Emissions from human breath ensured that isoprene was always present in our model runs. However, its removal rate varied with the air exchange rate, which affected the concentrations of ozone and hydroxyl radicals (which can both chemically remove isoprene), and the direct removal rate by ventilation. Finally, we used our results to understand the 95% confidence bounds around our median predicted concentrations. For hydroxyl radicals, these were ±60% of the median value.

1. Introduction

It has been estimated that in developed countries, we spend approximately 90% of our time indoors (i.e. at home, in the work place or commuting) and consequently, this is where most of our exposure to air pollution occurs (Carslaw, 2007). Despite this fact, most of the regulation around exposure to air pollution focuses on the outdoor environment. Indoor air quality issues are becoming increasingly topical. Compared to seventy years ago, we are spending more time indoors, in buildings that have better insulation owing to increased

* Corresponding author.
E-mail address: nicola.carslaw@york.ac.uk (N. Carslaw).

https://doi.org/10.1016/j.atmosenv.2021.118625
Received 19 May 2021; Received in revised form 9 July 2021; Accepted 14 July 2021
Available online 21 July 2021

energy efficiency measures. Over the same time period, we have become an increasingly consumer-driven society bringing more items into our homes (and other buildings) that emit an ever increasing and varying mixture of indoor air chemicals (Weschler, 2009). As a result, we are spending more of our time in increasingly airtight buildings and with higher internal emissions (Weschler and Carslaw, 2018). During the COVID-19 pandemic has led populations in many countries to spend even more time in their homes, owing to the various lockdown measures in place.

Indoor air quality is recognised as a multi-disciplinary phenomenon and can be affected by many chemical (e.g. emissions from personal care and cleaning products, furnishings and building materials, and products from chemical reactions), physical (temperature, humidity, light levels) and building (location, ventilation regime, building operation) factors (Tham, 2016). Indoor air pollutants are generated through activities such as cooking, cleaning and smoking, as well as emitted from building materials like painted walls and ceilings, furnishing and consumer products such as cleaning agents, air fresheners and personal care products (Nazaroff and Weschler, 2004; Carslaw et al., 2012). As well as indoor emissions, indoor air pollutants can ingress from outdoors and indoor environments often contain higher concentrations of some air pollutants than outdoors (Brown, 2002; Wolkoff et al., 2013).

Once indoors, ozone can initiate a wide range of indoor air chemistry (Weschler and Carslaw, 2018). For instance, ozone-initiated reactions with double-bonded species such as terpenes in the gas-phase, as well as heterogeneous interactions with indoor surfaces, can contribute to the formation of secondary pollutants (Weschler and Carslaw, 2018; Weschler, 2011; Wolkoff, 2013; Kruza et al., 2017; Carslaw and Shaw, 2019). There is also increasing evidence that the presence of human occupants indoors is highly correlated with ozone loss and enhanced secondary pollutant formation (Wisthaler and Weschler, 2010; Kruza and Carslaw, 2019; Liu et al., 2021). Furthermore, some of these secondary pollutants are likely to be harmful to human health (Weschler and Carslaw, 2018).

Clearly then, the indoor environment is both physically and chemically complex and we need to better understand it if we wish to gain a more holistic view of an individual's exposure to air pollution. One way to gain this insight is to make measurements of the species that exist in indoor air for typical buildings. However, identifying the numerous different chemical species that exist indoors is challenging, as is quantifying the concentrations of many of them analytically (Terry et al., 2014). It is also hard to define what a typical building is, as occupant behaviour is an important driver for indoor air pollutant concentrations (Weschler and Carslaw, 2018). Given all of these factors, models are often used to predict indoor air concentrations over a wide range of conditions and to provide insight into the underlying chemical processing.

This paper uses a detailed chemical model for indoor air chemistry, to evaluate the controlling factors for predicted indoor air concentrations in a typical residence. A Monte Carlo simulation study is used to investigate the key controlling factors for the predicted concentrations of several key indoor species to identify which of these factors are most important. The impact of varying these factors on model output are also explored. In this way, we identify the major model uncertainties that exist and suggest which of these need to be addressed most urgently to improve model predictions in the future.

2. Methods

2.1. The INDCM model overview

The INDCM is a near explicit box model used for studying indoor air chemistry (Carslaw, 2007; Carslaw et al., 2012). It uses a comprehensive chemical mechanism called the Master Chemical Mechanism (MCM v3.3.1) (Jenkin et al., 1997; Jenkin et al., 2003; Saunders et al., 2003) and involves the degradation of 143 volatile organic compounds (VOCs). The degradation process of VOCs is initiated by reactions with ozone (O_3), OH (hydroxyl) radicals, nitrate (NO_3) radicals and photolysis where relevant. Radicals, such as oxy (RO) and peroxy (RO_2) radicals, excited and stabilized Criegee (R'R"COO) species, are generated as intermediate products, as well as longer-lived species such as carbonyls, alcohols and organic nitrates. Eventually, water and carbon dioxide are produced at the end of the oxidation chain. The MCM also includes an inorganic scheme including reactions of O_3, nitrogen oxides (NO_x) and carbon monoxide (Jenkin et al., 1997, 2003, 2003; Saunders et al., 2003). The INDCM also includes terms that represent photolysis (both indoor lighting and attenuated sunlight), deposition onto surfaces and indoor-outdoor exchange (Carslaw, 2007). A detailed description of the model has been presented elsewhere (Carslaw, 2007; Carslaw et al., 2012; Kruza et al., 2017). Recently the INDCM has been developed to investigate surface interactions indoors (Kruza et al., 2017), the impact of cleaning with chlorine (Wong et al., 2017), the impact of occupancy on indoor air chemistry (Kruza and Carslaw, 2019), and gas-to-particle partitioning for α-pinene oxidation (Kruza et al., 2020). The modified INDCM includes ≈5900 species and ≈20,300 gas-phase reactions.

2.2. Baseline model run input parameters

The first stage in this study was to define baseline conditions. These are based on previous studies where we simulated an apartment in Milan in summertime (Kruza et al., 2017) and just serves as a background against which to compare our Monte Carlo results. It is not the purpose of this work to replicate experimental results indoors, which we have done extensively in the past (e.g. Carslaw et al. (2017); Zhou et al. (2020); Wong et al. (2017)). The apartment is assumed to have a volume of 168 m^3 and surface to volume ratio of ≈2.0 m^{-1}. The surface to volume ratio is determined by the indoor dimensions: surface coverings, and furnishing, such as hard furniture together with internal doors (22 m^2), soft furniture (35 m^2), wooden floors (51 m^2), painted walls and ceilings (199 m^2), linoleum including in the kitchen and bathrooms (11 m^2) and countertops and tiled surfaces, including those in the kitchen and bathroom (19 m^2). It is assumed that two adults were in the household, with a surface area of 2 m^2 each. A detailed description of the case study apartment and the origin of these assumptions can be found in Kruza et al. (2017).

Secondary product emissions following ozone deposition onto each type of internal surface are treated as described by Kruza et al. (2017) and Kruza and Carslaw (2019). The ozone deposition velocity onto soft furniture is assumed to be 0.15 cm s^{-1}, 0.007 cm s^{-1} for linoleum, 0.026 cm s^{-1} for painted walls, 0.005 cm s^{-1} for wooden furniture, 0.069 cm s^{-1} for wooden floors, 0.136 cm s^{-1} for countertops/tiled surfaces and 0.285 cm s^{-1} for skin, based on median values (Kruza et al., 2017). The aldehyde yields following ozone deposition and the emissions from exhaled human breath were calculated following the methodology presented by Kruza et al. (2017) and Kruza and Carslaw (2019).

The baseline model run assumed a temperature of 297.07 K, a relative humidity of 50% and an air exchange rate of 0.72 h^{-1} based on a literature evaluation of typical indoor values observed across a range of residences (Weisel et al., 2005; Colton et al., 2014; Williams et al., 2009; Johnson et al., 2004; Zhu et al., 2005; Zota et al., 2005; Less et al., 2015; Hodgson et al., 2000; Arhami et al., 2009; Gilbert et al., 2005; Chao, 2001; Jo and Lee, 2006). We also assumed that 49.2% of visible light and 14% of UV light was able to pass through the windows and enter the room based on the median values for the UV and visible light transmission data reported by Blocquet et al. (2018) for a series of windows including their own measurements, plus data reported by Gandolfo et al. (2016), Kim and Jeong Tai Kim (2010) and Sacht et al. (2016). Outdoor concentrations of O_3, NO_2, NO (nitric oxide) and particulate matter ($PM_{2.5}$) were taken from the typical summer time period in Milan and were based on the values available from Terry et al. (2014). The VOC concentrations were set at constant values outdoors as detailed in Kruza and Carslaw (2019). Indoor VOC emissions were taken from Sarwar

et al. (2002) and Zhu et al. (2013).

The baseline simulation was run from 8am on day one until midnight on day two and all analysis was performed on the results from day two, to allow time for the simulated concentrations to reach steady-state. The day two indoor concentrations for OH, ozone, NO, and NO_2 for the baseline scenario are plotted in Fig. 1 and show the diurnal variation for each species, with daily-averaged concentrations and mixing ratios of 3.9×10^5 molecules cm^{-3}, 5.7 ppb, 1.7 ppb, and 7.9 ppb respectively.

2.3. Individual sensitivity analysis

In order to sift the numerous model inputs for importance, an individual sensitivity analysis was first carried out. This involved running simulations for the maximum and minimum values for a range of key input parameters individually, while maintaining baseline values for all others. The following parameters were varied based on their distributions from the same sources used to define the median values for the baseline model run in section 2.2: ozone deposition velocities for 7 different surfaces, secondary product formation yields for 3–5 aldehydes from relevant surfaces, attenuated sunlight (as a %) passing indoors in the UV and visible wavelength regions, air exchange rate, internal temperature and relative humidity and VOC emission rates from exhaled breath. Twenty key rate coefficients for reactions between key VOCs and OH and ozone (if relevant) were varied within their started uncertainty bounds as shown in Table ST1 in the Supplementary Information. The surface to volume ratios of each type of surface, as well as the total surface area, were varied within ±10% of their baseline values. Outdoor ozone, NO, NO_2 and particulate matter concentrations were varied from half their baseline values, to the concentrations experienced during a polluted episode during the summer of 2003 (Terry et al., 2014). The maximum and minimum values of all input parameters investigated apart from the rate coefficients are shown alongside baseline values in Table ST2 in the supplementary information accompanying this paper. This resulted in a total of 111 individual simulations.

The outputs were examined to discover the impact of the maximum and minimum parameter values on the indoor concentrations of ozone, NO_2, NO, OH, HO_2, RO_2, nitrous acid (HONO), total suspended particles, formaldehyde, limonene, α-pinene, hexanal, heptanal, octanal, nonanal, decanal, 4-oxopentanal, formic acid, acetic acid, acetone, methanol, ethanol, isopropanol and isoprene. These species reflect a range of lifetimes (from seconds to days) and sources (e.g. from cleaning, people, outdoors, surface interaction, chemical reactions), providing a good sense of overall model sensitivity to the input parameters. Where the sensitivity test results showed a minimum of 10% difference in the predicted daily-averaged concentrations of any of the identified 24 species compared to the baseline run results, that particular input was selected for the more comprehensive Monte Carlo analysis in the next section. This process identified the following input parameters for further analysis: secondary product formation yields following ozone interaction with soft furniture (for hexanal, heptanal, octanal, nonanal and decanal) and painted walls (for octanal, nonanal and decanal), the surface to volume ratio for soft furniture, painted walls, linoleum, countertops, skin and the total surface to volume ratio, the ozone deposition velocity onto soft furniture and painted walls, the air exchange rate, the temperature, the % of UV light that ingressed through the windows and the isoprene emission rate from human breath.

2.4. Monte Carlo analysis

The 20 model input parameters identified in the previous section were stochastically assigned to values between the maximum and minimum value from their distributions as shown in Table 1. The value assignment for individual runs was carried out using the uniform function from the random Python library which gives an equal probability of any value within the given interval being chosen. Although using the Mersenne Twister as the core generator is technically pseudo-random, it is a method that is perfectly suited for this purpose (Matsumoto and

Table 1
Minimum and maximum values of the 20 input parameters used for the Monte Carlo analysis.

Parameter	Minimum value input	Maximum value input
Hexanal yield from soft furniture	0	0.08
Heptanal yield from soft furniture	0	0.04
Octanal yield from soft furniture	0	0.07
Nonanal yield from soft furniture	0	0.14
Decanal yield from soft furniture	0	0.09
Octanal yield from painted walls	0	0.03
Nonanal yield from painted walls	0	0.34
Decanal yield from painted walls	0	0.12
Soft furniture surface to volume ratio (cm^{-1})	0.0019	0.0023
Painted wall surface to volume ratio (cm^{-1})	0.0106	0.0130
Linoleum surface to volume ratio (cm^{-1})	0.0006	0.0007
Countertop surface to volume ratio (cm^{-1})	0.001	0.0012
Human body surface to volume ratio (cm^{-1})	0.0002	0.0003
Total surface to volume ratio (cm^{-1})	0.0182	0.0222
Ozone soft furnishings deposition velocity (cm s^{-1})	0.04	0.19
Ozone painted wall deposition velocity (cm s^{-1})	0.01	0.17
Internal temperature (K)	295.18	298.85
Air exchange rate (h^{-1})	0.43	1.34
Emission rate of isoprene from breath (molecules cm^{-3} s^{-1})	6.41×10^5	3.1×10^7
UV light transmission (%)	0	38

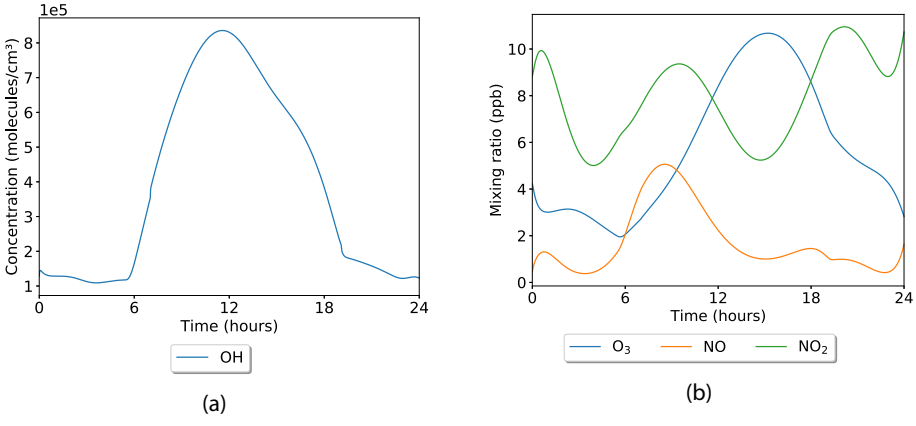

Fig. 1. OH (a) and O_3, NO_2, and NO (b) concentrations for day two of the baseline model run.

Nishimura, 1998). There was no relation between the random assignment of one parameter and another and thus the combination of parameters for each simulation was also randomised. This process was used to produce 1000 model simulations in which these 20 input parameters were varied randomly across their potential range of values and the impact on model output explored in the next section.

3. Results

Outputs from the model were analysed as predicted daily-averaged species concentrations on day 2 versus single varied input parameters. As the trends were non-linear, correlation was quantified by calculating a Spearman's rank correlation coefficient for each input parameter and a selected species concentration (Spearman, 1904), which is shown in Fig. 2. These coefficients allow for the general trends and sensitivities to be inferred. A positive coefficient indicates an increase in the species concentration as the input parameter value increases (red in Fig. 2), whilst the converse is true for a negative coefficient (blue in Fig. 2). The closer the absolute value of the coefficient is to 1, the stronger the correlation. Values close to 0 show almost no correlation between the variation in input parameter and the concentration of the output species.

From Fig. 2 there are obvious important inputs, such as the air exchange rate, transmission of UV light indoors and the ozone deposition velocity on painted walls, which show high correlation for many of the key species shown. Some parameters show significant correlation for only one species. For instance, varying the octanal yield from painted walls following ozone interaction only affects the predicted octanal concentration. Interestingly, increasing the decanal production yield from painted walls increases the concentration of decanal as expected, but also leads to reduced concentrations of octanal and nonanal, presumably as less ozone is then available to interact with the surface and produce the latter two species. Not surprisingly, the predicted concentration of isoprene shows a strong correlation with its emission rate from breath.

Looking in more detail, there is a strong positive correlation between ethanol (C_2H_5OH) and the air exchange rate as shown in Fig. 3. In the absence of specific indoor sources of ethanol, the concentration is controlled through exchange with outdoors and thus increases with the air exchange rate almost linearly. At higher air exchange rates, there will

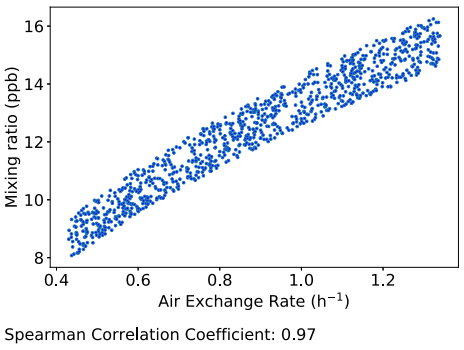

Fig. 3. Ethanol concentration as a function of the air exchange rate.

be more indoor ozone ingress from outdoors and hence more hydroxyl radicals produced indoors through ozone chemistry (Weschler and Carslaw, 2018). The OH radicals can react with ethanol albeit slowly, so this explains why the increase in ethanol concentrations flattens off slightly as the air exchange rate increases.

In Fig. 4, a very different pattern can be seen for the isoprene concentration variation with air exchange rate. The maximum concentration of isoprene (C_5H_8) decreases with the air exchange rate while the

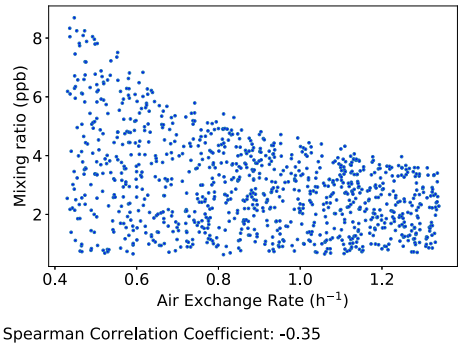

Fig. 4. Isoprene as a function of the air exchange rate.

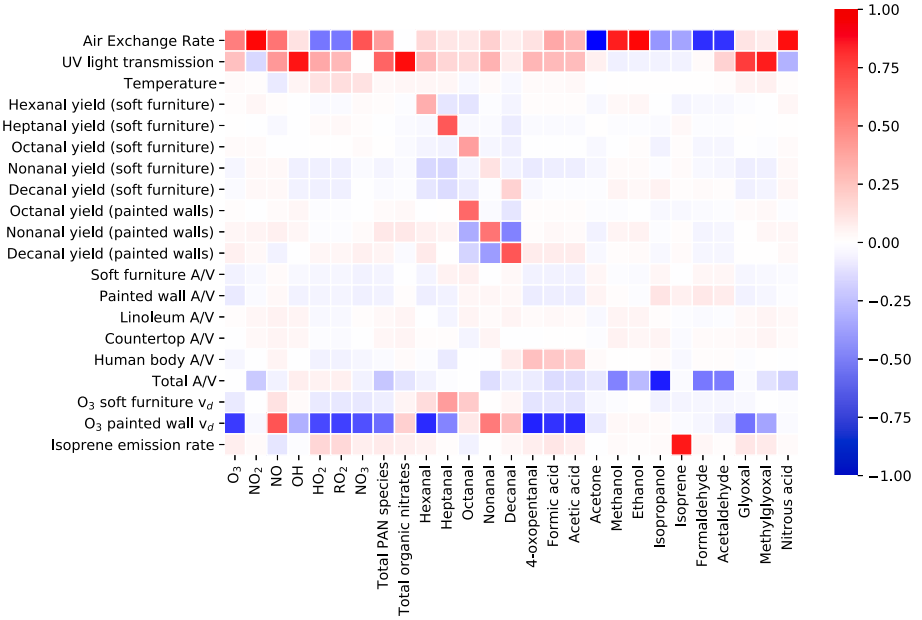

Fig. 2. Spearman's rank correlation coefficients between input variables and output concentrations. The colour scale on the right indicates the strength of the positive and negative correlations. A/V is the surface area to volume ratio, v_d is the deposition velocity and the isoprene emission is from breath. (For interpretation of the references to colour in this figure legend, the reader is referred to the Web version of this article.)

minimum concentration is largely unaffected. In contrast to ethanol, isoprene has an indoor source (from breath) and thus will always be present indoors with occupants. Isoprene can accumulate at lower air exchange rates. This is because the emissions from breath are not diluted as quickly under these conditions, but removal by ozone is also less important at the lower exchange rates, given ozone ingresses from outside. As the air exchange rate increases, so does the dilution rate and the removal rate by ozone. The spread of the data therefore decreases as the air exchange rate increases and the maximum indoor isoprene concentration converges with the outdoor concentration.

Fig. 5a shows the relationship between ozone concentration indoors and air exchange rate (a) and ozone deposition velocity onto painted walls (b). The ozone concentration increases almost linearly with the air exchange rate as expected. However, as ozone is intricately involved in many reactions and so depends at least partially on the concentrations of other species, there are more scattered maximum values when compared to the minimum values. Ozone is involved in 233 reactions as a reactant within the model and thus the accuracy of its concentration has a wide impact on other concentrations within the model, and vice versa. This is clear in Fig. 2 with many species showing strong correlations with the ozone deposition velocity onto walls.For ozone the highest correlation is with the deposition velocity onto painted walls which is shown in Fig. 5b. The spread of the ozone concentrations only decreases slightly as the deposition velocity increases and is smaller than for the air exchange rate relationship. In all cases where there is a strong correlation, by obtaining and inputting a more accurate measurement of a parameter there will be a noticeable reduction in the potential variation in the simulated concentration. For instance, for the case of ozone deposition velocity onto painted walls, by narrowing the deposition velocity to between 0.161 and 0.17 cm s^{-1} the range of potential predicted ozone concentrations reduces by 68%. Similarly, at the other end of the scale a narrowing to between 0.009 and 0.016 cm s^{-1} reduces the range of simulated concentrations by 33%. Therefore a reduction in the uncertainty in the predicted ozone concentration of between 33% and 68% can be achieved by having a more precise value for the deposition velocity onto painted walls.

Fig. 2 shows that there is a strong correlation between the OH concentration and the transmission of UV light. This relationship is explored in more detail in Fig. 6. OH has a very weak correlation with the other input variables, despite being involved in 4028 reactions in the model and having at least some measure of dependency on the concentrations of many other species. Transmission of UV light will therefore also be important for many of the other species that OH reacts with, or which are created from an OH reaction. By narrowing the UV light transmission variable to absolute values between 0 and 2% the range of potential OH concentrations decreases by 80%. By narrowing the UV photolysis absolute value to between 36 and 38% the range of potential concentrations decreases by 51%. Thus a reduction in the uncertainty around the UV light transmission variable will increase the accuracy of the OH

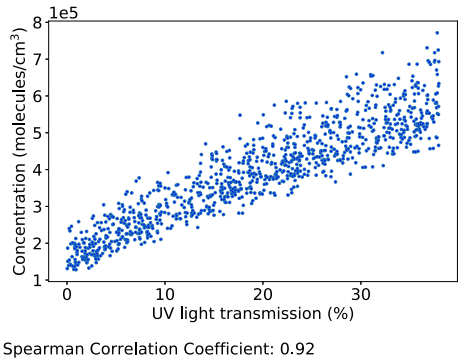

Fig. 6. OH concentration with the UV attenuation factor.

predicted concentration from the model by 51–80%.The radicals OH, HO_2 and RO_2 have mechanistic links with ozone, which are represented in the correlations shown in Fig. 2. The weak positive correlations with transmission of UV light for HO_2 and RO_2 (0.34 and 0.28 respectively) can be attributed to the numerous production routes for these radicals from OH, which has a strong correlation with UV light transmission as discussed above. Shown in Fig. 7 are HO_2 and RO_2 correlations with the air exchange rate (−0.53 and −0.52 respectively) and the ozone deposition velocity onto painted walls (−0.72 and −0.75 respectively). HO_2 and RO_2 are produced from ozone and OH reacting with VOCs (Sarwar et al., 2002; Carslaw and Shaw, 2019). Their highest predicted concentrations are typically for simulations where the ozone deposition velocity onto painted walls is low and hence ozone concentration is high and it is readily available to react. However, we also know that ozone increases with the air exchange rate, so we might also expect HO_2 and RO_2 to increase, but Fig. 7 shows the opposite occurs. This can be explained by the NO concentrations shown in Fig. 8: NO also increases with the air exchange rate given it derives from outdoors in these simulations and it reacts with the HO_2 and RO_2 and reduces their concentrations. There is clearly much interconnected and complex chemistry occurring.

Using the outputs from the Monte Carlo simulation, it is possible to determine a 95% confidence interval for each species when input variables lie within the bounds used within this study. These are presented in Table 2 alongside the median species concentration. The median value is preferred to the mean as all of the species concentrations give non-normal density functions and some are bi-modal, as shown in the distribution plots in figures S1-S27 in the Supplementary Information. Some distributions show high degrees of skew (e.g. hexanal as shown in figure S2) whilst other species have close to normal distributions (e.g. nonanal as shown in figure S6). Consequently, the median value better represents the distribution of the data. So for our two examples, the predicted median mixing ratio and the 95% confidence interval for

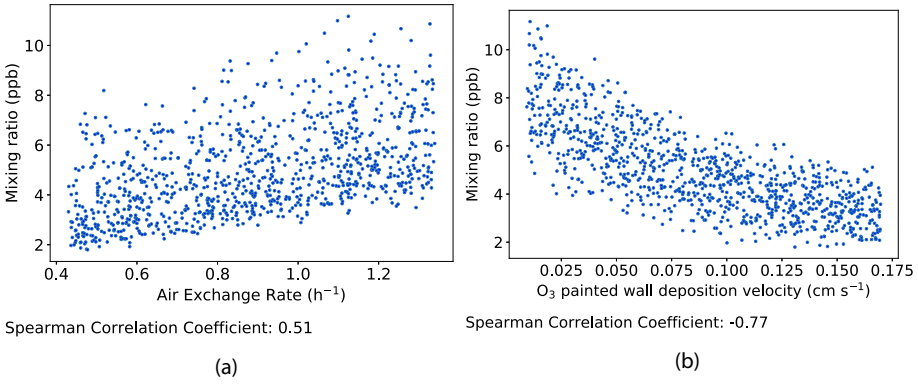

Fig. 5. (a) Ozone concentration as a function of air exchange rate and (b) ozone concentration as a function of ozone deposition velocity onto painted walls.

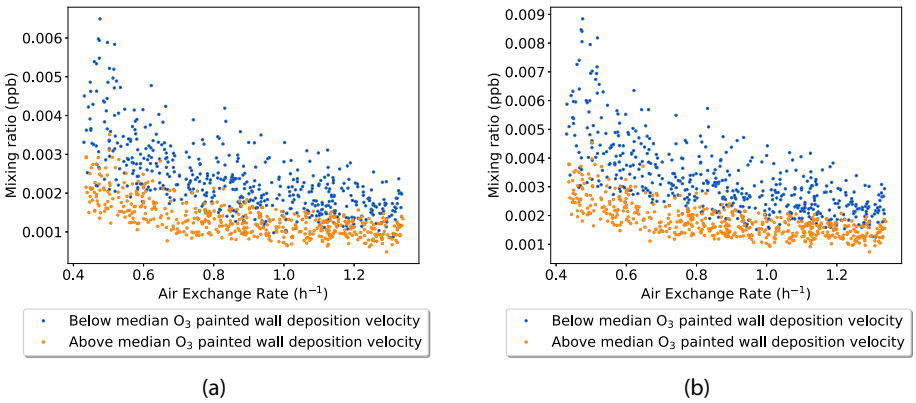

Fig. 7. HO_2 (a) and RO_2 (b) concentrations as a function of the air exchange rate. The data in blue are simulations with an ozone deposition velocity below the median of all values and the orange data has above median values of ozone deposition velocity. (For interpretation of the references to colour in this figure legend, the reader is referred to the Web version of this article.)

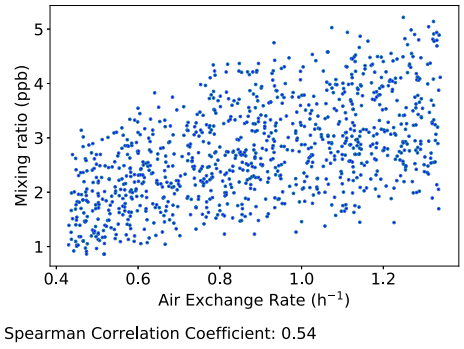

Fig. 8. NO concentration as a function of air exchange rate.

nonanal is $9.2^{+5.8}_{-5.4}$ ppb, whilst for hexanal, it is $2.2^{+2.0}_{-0.9}$ ppb.

Finally, we investigated the input conditions that gave the maximum concentrations of each of our individual species in the 1000 model outputs. For each run that produced a maximum concentration for one (or more) of the investigated species, we graded each of the varied input parameters for that run according to where it sat within the range of possible values for that input parameter (figure S28, SI). So if it was close to the maximum value in the input range it was coloured dark red, and dark blue if close to the minimum value. Not surprisingly, this exercise showed that the highest predicted ozone concentration was associated with a low deposition velocity of ozone onto painted walls.

The highest concentrations of NO_2 and HONO were associated with a run that had very low UV transmission and hence, lower photolysis rates for these two species. This latter relationship is shown in Fig. 9, which

Table 2
95% confidence bounds and median values for output species concentrations. These are shown graphically on density functions for each species in the supplementary information accompanying this paper.

Species	Median	Minimum bound	Maximum bound
O_3 (ppb)	4.7	2.3	9.1
NO_2 (ppb)	9	5.3	12
NO (ppb)	2.7	1.1	4.6
OH (molecules cm^{-3})	4×10^5	1.6×10^5	6.4×10^5
HO_2 (ppb)	0.0016	0.00078	0.0043
RO_2 (ppb)	0.0022	0.0011	0.006
NO_3 (ppb)	1.7×10^{-6}	5.5×10^{-7}	4.4×10^{-6}
Total PAN species (ppb)	0.46	0.22	0.76
Total organic nitrates (ppb)	0.29	0.094	0.58
Hexanal (ppb)	2.2	1.3	4.2
Heptanal (ppb)	0.39	0.18	1
Octanal (ppb)	1.2	0.41	3.2
Nonanal (ppb)	9.2	3.8	15
Decanal (ppb)	2.9	0.75	8.8
4-oxopentanal (ppb)	0.08	0.047	0.15
Formic acid (ppb)	0.011	0.0061	0.022
Acetic acid (ppb)	0.012	0.0065	0.021
Acetone (ppb)	8.7	7.3	12
Methanol (ppb)	1.7	1.4	2
Ethanol (ppb)	13	8.7	16
Isopropanol (ppb)	0.88	0.83	0.96
Isoprene (ppb)	2.8	0.77	6.7
Formaldehyde (ppb)	18	16	21
Acetaldehyde (ppb)	4.1	3.8	4.6
Glyoxal (ppb)	0.35	0.18	0.5
Methylglyoxal (ppb)	0.071	0.031	0.11
Nitrous acid (ppb)	0.56	0.35	0.73

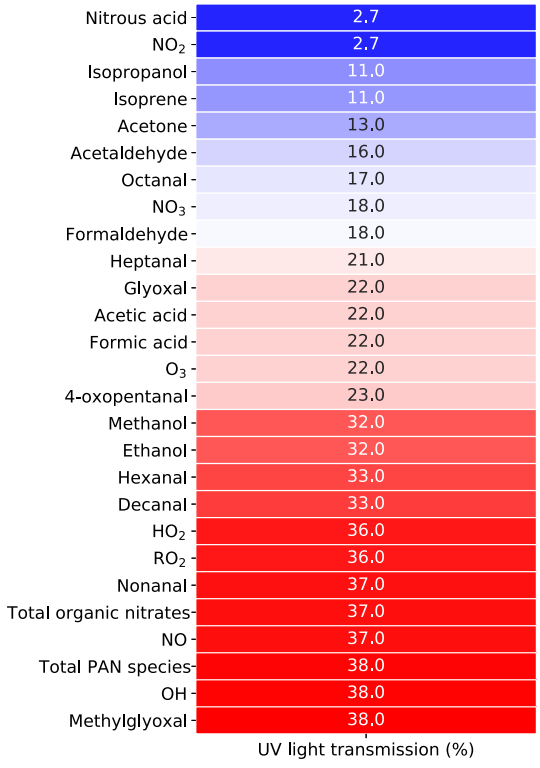

Fig. 9. Heatmap showing UV transmission values for simulations with maximum concentrations of each species. UV transmission had a minimum parameter value of 0% and a maximum of 38%.

ranks the importance of UV transmission for each of the species in the run that provides their maximum concentrations. It is interesting that potentially harmful species are present at both ends of the scale. Although increasing UV transmission indoors might decrease NO_2 and HONO concentrations, it would also likely increase the concentrations of PAN species and organic nitrates, both also with likely health impacts (Carslaw and Shaw, 2019).

4. Conclusions

This paper has shown that the model predicted concentrations of several key indoor air species are sensitive to a number of factors, particularly to ozone deposition velocity onto different surfaces, the C_6–C_{10} aldehyde formation yields, the ingress of UV light, the air exchange rate, temperature, humidity, the total surface to volume ratio as well as those for specific surfaces and VOC emission rates from breath. When these different input parameters were combined in a Monte Carlo sensitivity analysis, the air exchange rate and the ozone deposition velocity onto painted walls showed the highest correlations with most of the predicted species concentrations, such as ozone, RO_2 and HO_2 radicals. The ingress of UV light showed the strongest correlation with the predicted concentrations of OH and also with organic nitrate concentrations. This finding suggests that reducing the uncertainty in these input parameters will have the biggest impact on reducing model uncertainty and highlights future experimental research needs. This finding suggests that reducing the uncertainty in these input parameters will have the biggest impact on reducing model uncertainty, at least for the conditions we studied. Clearly, if there are activities involved that release emissions of particular air pollutants (e.g. cooking, cleaning, or surface chemistry), such an analysis might produce different conclusions. However, our results should be generally applicable for background conditions in a typical house.

This research also highlights future experimental research needs, which fall into two different areas. The first is a list of experimental parameters that must be measured when indoor air measurements are made, in order to gain further insight from later modelling studies. These include parameters such as the air exchange rate and transmission of UV light. The second area is where measurements under controlled conditions in an experimental laboratory could be useful to determine the properties of different surfaces indoors and in particular, how ozone interacts with them. As shown by Kruza et al. (2017), there is currently much variation in the reported values of ozone deposition velocities onto different surfaces and even onto the same surface types.

Finally, there is a need to acknowledge that we can only include in models, the processes that we know about at any point in time. We are still learning much about indoor air chemistry, particularly the impacts of the human occupant (e.g. Weschler and Carslaw (2018)) and of internal surfaces (e.g. Liu et al. (2021)). Attempting to parameterise these processes in indoor models is still at a very early stage and will no doubt raise some interesting challenges for modellers in the coming years.

Data availability

Data from this project is available at https://doi.org/10.15124/7464549f-f3ab-4c29-9473-7735b400cae0, an online data repository hosted by the University of York (Kruza et al., 2021).

CRediT authorship contribution statement

Magdalena Kruza: Conceptualization, Methodology, Software, Validation, Investigation, Writing – original draft. **David Shaw:** Software, Validation, Formal analysis, Investigation, Data curation, Writing – original draft, Writing – review & editing, Visualization. **Jacob Shaw:** Investigation, Data curation. **Nicola Carslaw:** Conceptualization, Methodology, Software, Supervision, Writing – review & editing, Project administration, Funding acquisition.

Declaration of competing interest

The authors declare that they have no known competing financial interests or personal relationships that could have appeared to influence the work reported in this paper.

Acknowledgements

This research is part of MOCCIE (MOdelling Consortium for Chemistry of Indoor Environments), which has received funding from an Alfred P. Sloan Foundation program to study Chemistry of Indoor Environments (CIE) grant 2017-9796 and grant 2018-10083. Conclusions reached or positions taken by researchers or other grantees represent the views of the grantees themselves and not those of the Alfred P. Sloan Foundation or its trustees, officers, or staff.

Appendix A. Supplementary data

Supplementary data to this article can be found online at https://doi.org/10.1016/j.atmosenv.2021.118625.

References

Arhami, M., Polidori, A., Delfino, R.J., Tjoa, T., Sioutas, C., 2009. Associations between personal, indoor, and residential outdoor pollutant concentrations: implications for exposure assessment to size-fractionated particulate matter. J. Air Waste Manag. Assoc. 59, 392–404. https://www.tandfonline.com/doi/full/10.3155/1047-3289.59.4.392, 10.3155/1047-3289.59.4.392.

Blocquet, M., Guo, F., Mendez, M., Ward, M., Coudert, S., Batut, S., Hecquet, C., Blond, N., Fittschen, C., Schoemaecker, C., 2018. Impact of the spectral and spatial properties of natural light on indoor gas-phase chemistry: experimental and modeling study. Indoor Air 28, 426–440. https://doi.org/10.1111/ina.12450.

Brown, S.K., 2002. Volatile organic pollutants in new and established buildings in Melbourne, Australia. Indoor Air 12, 55–63. https://doi.org/10.1034/j.1600-0668.2002.120107.x, 10.1034/j.1600-0668.2002.120107.x.

Carslaw, N., 2007. A new detailed chemical model for indoor air pollution. Atmos. Environ. 41, 1164–1179. https://doi.org/10.1016/j.atmosenv.2006.09.038.

Carslaw, N., Fletcher, L., Heard, D., Ingham, T., Walker, H., 2017. Significant OH production under surface cleaning and air cleaning conditions: impact on indoor air quality. Indoor Air 27, 1091–1100. https://doi.org/10.1111/ina.12394, 10.1111/ina.12394.

Carslaw, N., Mota, T., Jenkin, M.E., Barley, M.H., McFiggans, G., 2012. A Significant role for nitrate and peroxide groups on indoor secondary organic aerosol. Environ. Sci. Technol. 46, 9290–9298. https://doi.org/10.1021/es301350x.

Carslaw, N., Shaw, D., 2019. Secondary product creation potential (SPCP): a metric for assessing the potential impact of indoor air pollution on human health. Environ. Sci.: Processes and Impacts 21, 1313–1322. https://doi.org/10.1039/c9em00140a.

Chao, C.Y., 2001. Comparison between indoor and outdoor air contaminant levels in residential buildings from passive sampler study. Build. Environ. 36, 999–1007. https://linkinghub.elsevier.com/retrieve/pii/S0360132300000573, 10.1016/S0360-1323(00)00057-3.

Colton, M.D., MacNaughton, P., Vallarino, J., Kane, J., Bennett-Fripp, M., Spengler, J.D., Adamkiewicz, G., 2014. Indoor air quality in green vs conventional multifamily low-income housing. Environ. Sci. Technol. 48, 7833–7841. https://pubs.acs.org/doi/10.1021/es501489u, 10.1021/es501489u.

Gandolfo, A., Gligorovski, V., Bartolomei, V., Tlili, S., Gómez Alvarez, E., Wortham, H., Kleffmann, J., Gligorovski, S., 2016. Spectrally resolved actinic flux and photolysis frequencies of key species within an indoor environment. Build. Environ. 109, 50–57. https://doi.org/10.1016/j.buildenv.2016.08.026.

Gilbert, N.L., Guay, M., David Miller, J., Judek, S., Chan, C.C., Dales, R.E., 2005. Levels and determinants of formaldehyde, acetaldehyde, and acrolein in residential indoor air in Prince Edward Island, Canada. Environ. Res. 99, 11–17. https://linkinghub.elsevier.com/retrieve/pii/S0013935104001872, 10.1016/j.envres.2004.09.009.

Hodgson, A.T., Rudd, A.F., Beal, D., Chandra, S., 2000. Volatile organic compound concentrations and emission rates in new manufactured and site-built houses. Indoor Air 10, 178–192. https://doi.org/10.1034/j.1600-0668.2000.010003178.x, 10.1034/j.1600-0668.2000.010003178.x.

Jenkin, M.E., Saunders, S.M., Pilling, M.J., 1997. The tropospheric degradation of volatile organic compounds: a protocol for mechanism development. Atmos. Environ. 31, 81–104. https://doi.org/10.1016/S1352-2310(96)00105-7.

Jenkin, M.E., Saunders, S.M., Wagner, V., Pilling, M.J., 2003. Protocol for the development of the Master Chemical Mechanism, MCM v3 (Part B): tropospheric degradation of aromatic volatile organic compounds. Atmos. Chem. Phys. 3, 181–193. https://acp.copernicus.org/articles/3/181/2003/, 10.5194/acp-3-181-2003.

Jo, W., Lee, J., 2006. Indoor and outdoor levels of respirable particulates (PM10) and Carbon Monoxide (CO) in high-rise apartment buildings. Atmos. Environ. 40, 6067–6076. https://linkinghub.elsevier.com/retrieve/pii/S1352231006005176, 10.1016/j.atmosenv.2006.05.037.

Johnson, T., Myers, J., Kelly, T., Wisbith, A., Ollison, W., 2004. A pilot study using scripted ventilation conditions to identify key factors affecting indoor pollutant concentration and air exchange rate in a residence. J. Expo. Sci. Environ. Epidemiol. 14, 1–22. http://www.nature.com/articles/7500294, 10.1038/sj.jea.7500294.

Kim, G., Kim, Jeong Tai, 2010. UV-ray filtering capability of transparent glazing materials for built environments. Indoor Built Environ. 19, 94–101. http://journals.sagepub.com/doi/10.1177/1420326X09358020, 10.1177/1420326X09358020.

Kruza, M., Carslaw, N., 2019. How do breath and skin emissions impact indoor air chemistry? Indoor Air 29, 369–379. https://doi.org/10.1111/ina.12539.

Kruza, M., Lewis, A.C., Morrison, G.C., Carslaw, N., 2017. Impact of surface ozone interactions on indoor air chemistry: a modeling study. Indoor Air 27, 1001–1011. https://doi.org/10.1111/ina.12381.

Kruza, M., McFiggans, G., Waring, M., Wells, J., Carslaw, N., 2020. Indoor secondary organic aerosols: towards an improved representation of their formation and composition in models. Atmos. Environ. 240, 117784. https://linkinghub.elsevier.com/retrieve/pii/S1352231020305161, 10.1016/j.atmosenv.2020.117784.

Kruza, M., Shaw, D., Shaw, J., Carslaw, N., 2021. Towards Improved Models for Indoor Air Chemistry: a Monte Carlo Simulation Study Dataset. https://doi.org/10.15124/7464549f-f3ab-4c29-9473-7735b400cae0.

Less, B., Mullen, N., Singer, B., Walker, I., 2015. Indoor air quality in 24 California residences designed as high-performance homes. Sci. Technol. Built. Environ. 21, 14–24. http://www.tandfonline.com/doi/abs/10.1080/10789669.2014.961850, 10.1080/10789669.2014.961850.

Liu, Y., Misztal, P.K., Arata, C., Weschler, C.J., Nazaroff, W.W., Goldstein, A.H., 2021. Observing ozone chemistry in an occupied residence. Proc. Natl. Acad. Sci. Unit. States Am. 118, e2018140118. URL: http://www.pnas.org/lookup/doi/10.1073/pnas.2018140118, 10.1073/pnas.2018140118.

Matsumoto, M., Nishimura, T., 1998. Mersenne twister. ACM Trans. Model Comput. Simulat 8, 3–30. https://dl.acm.org/doi/10.1145/272991.272995, 10.1145/272991.272995.

Nazaroff, W.W., Weschler, C.J., 2004. Cleaning products and air fresheners: exposure to primary and secondary air pollutants. Atmos. Environ. 38, 2841–2865. https://doi.org/10.1016/j.atmosenv.2004.02.040.

Sacht, H., Bragança, L., Almeida, M., Nascimento, J.H., Caram, R., 2016. Spectrophotometric characterization of simple glazings for a modular façade. Energy Procedia 96, 965–972. https://doi.org/10.1016/j.egypro.2016.09.175, 10.1016/j.egypro.2016.09.175.

Sarwar, G., Corsi, R., Kimura, Y., Allen, D., Weschler, C.J., 2002. Hydroxyl radicals in indoor environments. Atmos. Environ. 36, 3973–3988. URL: https://linkinghub.elsevier.com/retrieve/pii/S1352231002002789, 10.1016/S1352-2310(02)00278-9.

Saunders, S.M., Jenkin, M.E., Derwent, R.G., Pilling, M.J., 2003. Protocol for the development of the Master Chemical Mechanism, MCM v3 (Part A): tropospheric degradation of non-aromatic volatile organic compounds. Atmos. Chem. Phys. 3, 161–180. URL: https://acp.copernicus.org/articles/3/161/2003/, 10.5194/acp-3-161-2003.

Spearman, C., 1904. The proof and measurement of association between two things. Am. J. Psychol. 15, 72–101. https://doi.org/10.1037/h0065390.

Terry, A.C., Carslaw, N., Ashmore, M., Dimitroulopoulou, S., Carslaw, D.C., 2014. Occupant exposure to indoor air pollutants in modern European offices: an integrated modelling approach. Atmos. Environ. 82, 9–16. URL: https://linkinghub.elsevier.com/retrieve/pii/S1352231013007309, 10.1016/j.atmosenv.2013.09.042.

Tham, K.W., 2016. Indoor air quality and its effects on humans—a review of challenges and developments in the last 30 years. Energy Build. 130, 637–650. URL: https://linkinghub.elsevier.com/retrieve/pii/S0378778816307812, 10.1016/j.enbuild.2016.08.071.

Weisel, C.P., Zhang, J., Turpin, B.J., Morandi, M.T., Colome, S., Stock, T.H., Spektor, D.M., Korn, L., Winer, A., Alimokhtari, S., Kwon, J., Mohan, K., Harrington, R., Giovanetti, R., Cui, W., Afshar, M., Maberti, S., Shendell, D., 2005. Relationship of Indoor, Outdoor and Personal Air (RIOPA) study: study design, methods and quality assurance/control results. J. Expo. Sci. Environ. Epidemiol. 15, 123–137. URL: http://www.nature.com/articles/7500379, 10.1038/sj.jea.7500379.

Weschler, C.J., 2009. Changes in indoor pollutants since the 1950s. Atmos. Environ. 43, 153–169. https://doi.org/10.1016/j.atmosenv.2008.09.044.

Weschler, C.J., 2011. Chemistry in indoor environments: 20 years of research. Indoor Air 21, 205–218. https://doi.org/10.1111/j.1600-0668.2011.00713.x.

Weschler, C.J., Carslaw, N., 2018. Indoor chemistry. Environ. Sci. Technol. 52, 2419–2428. URL: https://pubs.acs.org/doi/10.1021/acs.est.7b06387, 10.1021/acs.est.7b06387.

Williams, R., Rea, A., Vette, A., Croghan, C., Whitaker, D., Stevens, C., Mcdow, S., Fortmann, R., Sheldon, L., Wilson, H., Thornburg, J., Phillips, M., Lawless, P., Rodes, C., Daughtrey, H., 2009. The design and field implementation of the detroit exposure and aerosol research study. J. Expo. Sci. Environ. Epidemiol. 19, 643–659. URL: http://www.nature.com/articles/jes200861, 10.1038/jes.2008.61.

Wisthaler, A., Weschler, C.J., 2010. Reactions of ozone with human skin lipids: sources of carbonyls, dicarbonyls, and hydroxycarbonyls in indoor air. Proc. Natl. Acad. Sci. Unit. States Am. 107, 6568–6575. URL: http://www.pnas.org/cgi/doi/10.1073/pnas.0904498106, 10.1073/pnas.0904498106.

Wolkoff, P., 2013. Indoor air pollutants in office environments: assessment of comfort, health, and performance. Int. J. Hyg Environ. Health 216, 371–394. URL: https://linkinghub.elsevier.com/retrieve/pii/S1438463912001046, 10.1016/j.ijheh.2012.08.001.

Wolkoff, P., Larsen, S.T., Hammer, M., Kofoed-Sørensen, V., Clausen, P.A., Nielsen, G.D., 2013. Human reference values for acute airway effects of five common ozone-initiated terpene reaction products in indoor air. Toxicol. Lett. 216, 54–64. URL: https://linkinghub.elsevier.com/retrieve/pii/S0378427412013811, 10.1016/j.toxlet.2012.11.008.

Wong, J.P.S., Carslaw, N., Zhao, R., Zhou, S., Abbatt, J.P.D., 2017. Observations and impacts of bleach washing on indoor chlorine chemistry. Indoor Air 27, 1082–1090. https://doi.org/10.1111/ina.12402.

Zhou, S., Liu, Z., Wang, Z., Young, C.J., Vandenboer, T.C., Guo, B.B., Zhang, J., Carslaw, N., Kahan, T.F., 2020. Hydrogen Peroxide Emission and Fate Indoors during Non-bleach Cleaning: A Chamber and Modeling Study. https://doi.org/10.1021/acs.est.0c04702.

Zhu, J., Newhook, R., Marro, L., Chan, C.C., 2005. Selected volatile organic compounds in residential air in the city of ottawa, Canada. Environ. Sci. Technol. 39, 3964–3971. https://pubs.acs.org/doi/10.1021/es050173u, 10.1021/es050173u.

Zhu, J., Wong, S.L., Cakmak, S., 2013. Nationally representative levels of selected volatile organic compounds in Canadian residential indoor air: population-based survey. Environ. Sci. Technol. 47, 13276–13283. URL: https://pubs.acs.org/doi/10.1021/es403055e, 10.1021/es403055e.

Zota, A., Adamkiewicz, G., Levy, J.I., Spengler, J.D., 2005. Ventilation in public housing: implications for indoor nitrogen dioxide concentrations. Indoor Air 15, 393–401. https://doi.org/10.1111/j.1600-0668.2005.00375.x.